

International Conference on Computational Science, ICCS 2013

Retrospective cost optimization for adaptive state estimation, input estimation, and model refinement

Anthony M. D'Amato^a, Asad A. Ali^b, Aaron Ridley^c, Dennis S. Bernstein^{b,*}

^a*Ford Motor Company, Dearborn, MI, USA*

^b*Aerospace Engineering Department, University of Michigan, Ann Arbor, MI 48109, USA*

^c*AOSS Department, University of Michigan, Ann Arbor, MI 48109, USA*

Abstract

Retrospective cost optimization was originally developed for adaptive control. In this paper, we show how this technique is applicable to three distinct but related problems, namely, state estimation, input estimation, and model refinement. To illustrate these techniques, we give two examples. In the first example, retrospective cost model refinement is used with synthetic data to estimate the cooling dynamics that are missing from a model of the ionosphere-thermosphere. In the second example, retrospective cost adaptive state estimation is used with data from a satellite to estimate a solar driver in the ionosphere-thermosphere, with performance gauged by using data from a second satellite.

Keywords: Model refinement; state estimation; input estimation

1. Introduction

System theory encompasses several distinct but richly interrelated problems. These problems can roughly be categorized as control, estimation, and identification. The latter two problems are especially relevant to DDDAS (dynamic data-driven application systems), which uses adaptive measurement strategies to enhance the accuracy of model predictions.

In this paper we show how retrospective cost adaptive control provides the foundation for estimation and identification algorithms in the form of retrospective cost state estimation, retrospective cost input estimation, and retrospective cost model refinement. These techniques facilitate dynamic data-driven applications by enabling ensemble-free state and driver estimation as well as model refinement for attaining higher fidelity models.

2. Retrospective Cost Adaptive Control

Retrospective Cost Adaptive Control (RCAC). RCAC was developed for aerospace applications, such as noise and vibration control, control of aircraft under failure conditions (e.g., icing and wing damage), and spacecraft attitude control [1, 2, 3, 4]. The RCAC algorithm and associated theory are described in [5, 6, 7, 8, 9]. The basic idea behind RCAC is simple and intuitive. During control-system operation, RCAC collects and stores

*Corresponding author.

E-mail address: dsbaero@umich.edu.

performance data over a trailing window. RCAC then *re-optimizes* the control inputs used over the trailing window by minimizing a retrospective cost function. In a kind of “thought experiment,” RCAC asks itself, “What control values would have given me improved performance were I able to go back into the past and replace the actual past control inputs with different values?” Of course, the re-optimized control inputs cannot be used, but they can suggest how the controller can be modified so that the *future* performance is improved. This process of re-optimization and controller update comprises the adaptive control algorithm. In effect, RCAC learns from the past to do better in the future. A block diagram of the RCAC control law is shown in Figure 1(a), where the performance signal \hat{z} is used by RCAC to update the Adaptive Feedback Controller.

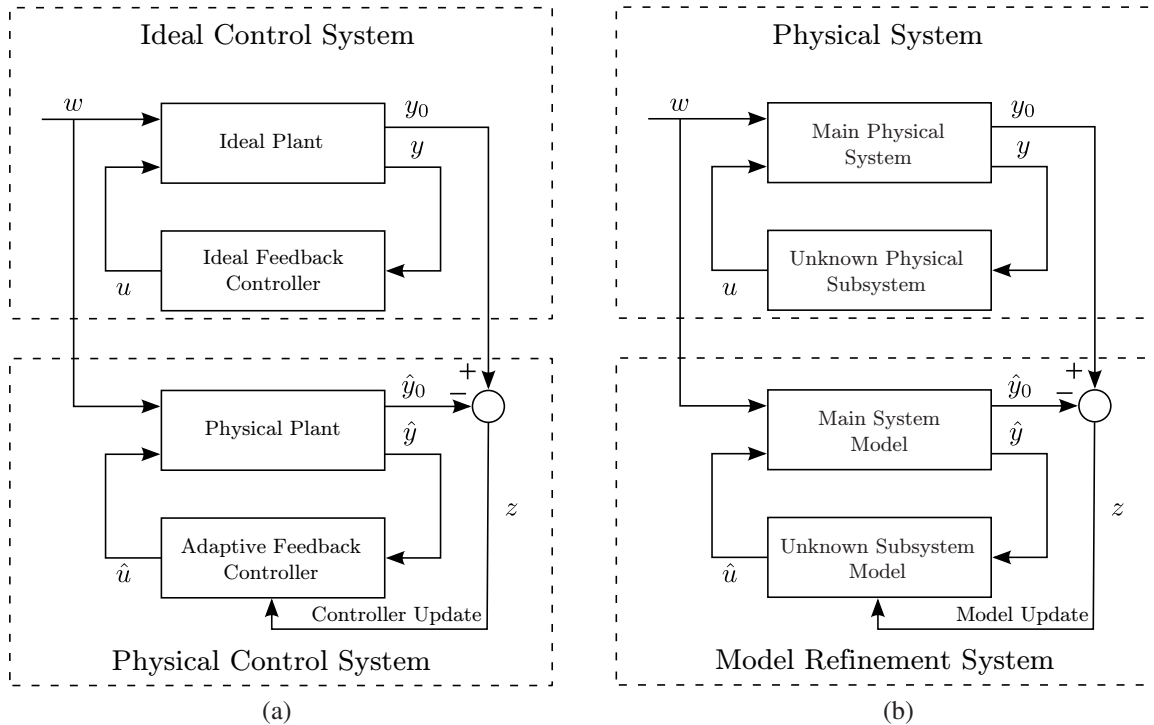


Fig. 1. These identical block diagrams illustrate the fact that, with appropriate signal reinterpretation, adaptive control and model refinement are essentially the same problem. In the case (a) of adaptive control, the Adaptive Feedback Controller is updated by RCAC so as to reduce the error variable z , which may represent, for example, an aircraft flight control or spacecraft attitude control objective. Since RCAC is an adaptive control algorithm, it uses minimal modeling information about the system it is controlling, and it can update the Adaptive Feedback Controller as needed in response to plant variations and unknown disturbances. In the case (b) of model refinement, the Unknown Subsystem Model is updated by RCMR as data are collected. Analogous to the case of adaptive control, RCMR updates the Unknown Subsystem Model so as to reduce the error variable z , which measures the discrepancy between the Physical System and the Model Refinement System. RCMR operates by estimating the inaccessible signal u in the Main Physical System; it then uses the estimate \hat{u} along with the computed output \hat{y} to update the Unknown Subsystem Model.

3. Retrospective Cost Model Refinement

It turns out, somewhat surprisingly, that RCAC can be used for an entirely different purpose. Specifically, by reinterpreting the signals and systems in the adaptive control problem, the same algorithm can be applied to model refinement in the form of retrospective cost model refinement (RCMR). To do this, we model the uncertain component of the system as an Unknown Physical Subsystem connected to the Main Physical System as shown in Figure 1(b). The goal of the Model Refinement System is to iteratively update the Unknown Subsystem Model

by using the error signal z . The relationship between model refinement and adaptive control is due to the fact that the Unknown Subsystem Model is exactly analogous to the Adaptive Feedback Controller.

A key feature of RCMR is its ability to use data to construct models of system components that are not accessible. In terms of Figure 1(b), this means that the interconnection signals y and u are not measured. To illustrate this point, think of diagnosing a spark plug in a car by operating only the gas pedal and measuring only the car's acceleration. RCMR thus has the ability to use *available* measurements to identify *inaccessible* subsystems. This ability is crucial in situations where physical measurements are limited and the drivers and response of poorly understood phenomena cannot be directly measured.

As shown in Figure 1, RCMR operates in the same way as RCAC except that the signals and operations have different interpretations. In the case of RCMR, the re-optimized input \hat{u} serves as an estimate of the output u of the Unknown Physical Subsystem. This estimate is used along with the computed signal \hat{y} from the Main System Model to update (through regression techniques) the estimate of the Unknown Physical Subsystem. The goal is to reduce the discrepancy between the Physical System and the Model Refinement System in the sense that the error based on the difference between the measured output y_0 and the computed output \hat{y}_0 is minimized. Just as RCAC learns from the past to do better in the future, RCMR uses data to learn about the Unknown Physical Subsystem, thereby enhancing the ability of the Main System Model and Unknown Subsystem Model to match the dynamics of the Physical System. Again, RCMR is virtually identical to RCAC in the sense that the computational techniques are the same but the results of the operations in the two cases are completely different. This conceptual insight is crucial to the multidisciplinary nature of the proposed research.

Within control systems research, system identification is widely used to provide models for controller analysis and synthesis [10, 11, 12, 13, 14, 15, 16]. RCMR belongs within this field, but provides a unique tool due to its ability to estimate an inaccessible subsystem. In contrast, system identification techniques generally aim to model the overall system rather than a targeted, unknown subsystem.

We have demonstrated RCMR using both experimental and simulated data. In laboratory test cases using real measurements, we used RCMR in [17] to estimate the parameters of an electronic circuit, while in [18] we used RCMR to update a model of a structural component. These experimental implementations of RCMR show its potential for working with physical measurements corrupted by noise. In addition, using synthetic (simulated) data from a truth model in [17], we used RCMR to estimate a thermal conductivity coefficient in the ionosphere.

4. Applicability to Nonlinear Systems

The derivation of the retrospective cost algorithm used by RCAC and RCMR is based on linear models. However, RCAC and RCMR have been demonstrated on a variety of nonlinear models. For example, RCAC has been used to control plants with input nonlinearities in [19], spacecraft with nonlinear rotational dynamics and attitude kinematics in [20], and diesel engines with nonlinear air flow dynamics in [21]. Likewise, RCMR has been used for model refinement and state estimation in nonlinear ionospheric dynamics [17, 22] and nonlinear battery dynamics in [23]. These examples demonstrate that RCAC and RCMR are effective for nonlinear systems. The effectiveness of RCMR for nonlinear systems is a consequence of the fact that the retrospective cost algorithm does not require an explicit model of the system being refined. Instead, RCMR is implemented with a single copy of the nonlinear system dynamics (which may be in the form of a computer code) and requires knowledge of extremely limited modeling information, namely, components of the impulse response; in many cases, only one component is needed. For the case of nonlinear systems, these impulse response parameters can be estimated based on the qualitative behavior of the system. In practice, this means that tuning RCMR typically requires selection of a single number. The sign of this number (positive or negative) must be correctly chosen, and the magnitude of this number can be adjusted to influence the convergence rate of the RCMR estimates of the Unknown Physical Subsystem.

5. Case Study: Retrospective Cost Model Refinement for GITM

We now present a case study in which the goal is to refine an initial model by estimating dynamics that are “missing” from the model. This objective supports the goals of DDDAS by enhancing model accuracy. The goal

of the study is to determine whether RCMR can provide an estimate of the Unknown Physical Subsystem corresponding to the NO cooling dynamics. For this purpose, the Main System Model is simply the GITM code without the NO cooling dynamics. The “missing” NO cooling dynamics are replaced by the Unknown Subsystem Model, which is the estimated NO cooling dynamics updated by RCMR. Figure 2 shows the output of the Unknown Subsystem Model estimated by RCMR. These results were obtained by implementing RCMR in FORTRAN within the context of GITM. For this study we use a 1D version of the Global Ionosphere-Thermosphere Model (GITM) [24, 25] to play the role of the Physical System to generate truth data for use by RCMR.

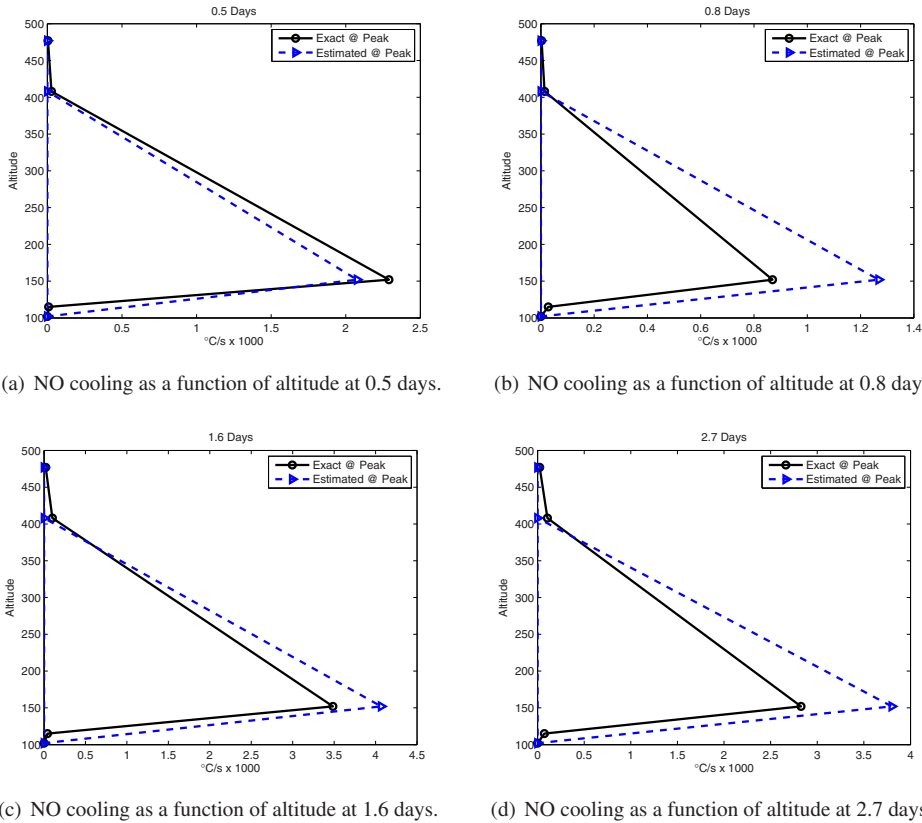
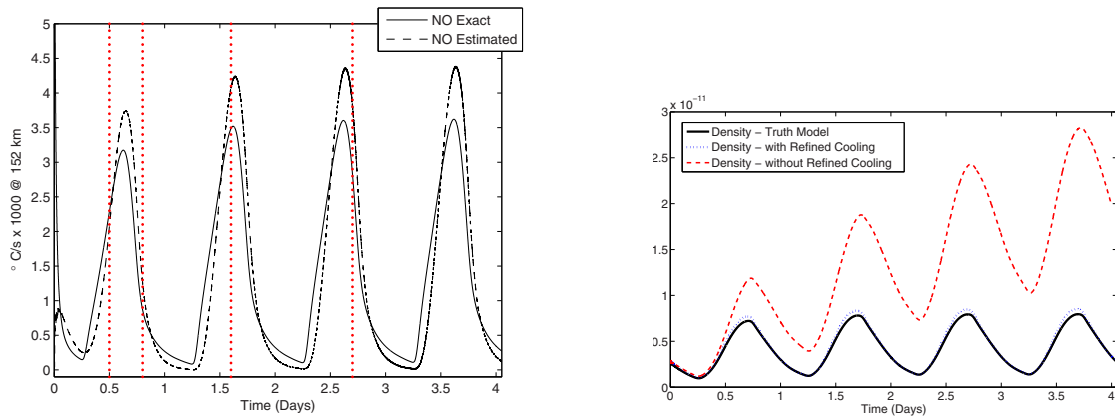


Fig. 2. In this example from [17], RCMR was used to construct a model of “missing physics,” namely, the nitrous oxide (NO) cooling dynamics in the GITM truth model of the ionosphere. The cooling rate at various altitudes and times is shown for a truth model playing the role of the Physical System; the same plots show the cooling rates for the Main System Model (that is, the truth model with the cooling dynamics removed) connected with the estimated Unknown Subsystem Model as updated by RCMR. These plots show the difference between the actual NO cooling included in the truth model and the cooling estimated by RCMR as a function of altitude at a given time. Cooling is along the horizontal axis, while altitude is along the vertical axis. The blue dashed line is the estimated value. To reflect conditions under which RCMR would be performed under real-world conditions, the data made available to RCMR consists of measurements of the thermospheric density at 407 km altitude, which for this study are obtained from the simulated GITM truth model (including NO cooling). The vertical dashed lines in Figure 2(a) are the time instances at which the altitude versus NO cooling plots (a)–(d) are taken. These plots indicate that RCMR has constructed a dynamic model that captures the Unknown Physical Subsystem Model of the “missing” cooling dynamics.

To reproduce the dynamics of the cooling, three linear dynamic equations are derived, one for each of the three chosen altitudes. This yields a profile that resembles the natural logarithm of the NO density [26, 27], indicating that this may be the source of the cooling, which it actually is. Figures 3(a) and 3(b) compare the model without correction versus the model with correction, both of which are baselined against the truth model. Without data-based model refinement, the estimated density measurements degrade as time increases.



(a) Comparison of truth and refined cooling models.

(b) Comparison of truth, refined, and “missing” cooling models.

Fig. 3. (a) shows the difference between the actual NO cooling included in the GITM truth model and the cooling in the refined GITM model as a function of time at a specific altitude (152 km). The vertical dashed lines are the time instances at which the altitude versus NO cooling plots in Figure 2 are taken. (b) shows the difference between the density measurements for the initial model, where no correction is made, and the model with the refined subsystem versus the truth model. With adaptive model refinement, the refined model is able to track the truth model, whereas, if no correction is made, the density measurements degrade as time increases.

6. Retrospective Cost Adaptive State Estimation

Although the objective of RCMR is to update the Unknown Subsystem Model, it also has the tendency to drive the internal states of the Main System Model toward the states of the Main Physical System. The states of the Main System Model thus serve as estimates of the states of the Main Physical System. Consequently, RCMR provides an *adaptive* technique for data assimilation as demonstrated in [28]. Retrospective cost adaptive state estimation (RCASE) was used for state and driver estimation within the context of a parallel implementation of 3D GITM in [22].

For data assimilation, RCMR does not propagate an estimate of the error covariance as in the case of particle and ensemble methods [29]. Rather, RCMR provides “point” estimates without an associated probability distribution. Consequently, for data assimilation, RCMR does not provide the depth of statistical insight that ensemble data assimilation methods provide; accordingly, it does not require any prior statistical information. In addition, since RCMR is based on an adaptive algorithm, it does not require an ensemble of models to propagate state estimates; this means that RCMR is highly computationally efficient. For example, for the simulations of RCMR in [22], a single copy of GITM (which is all that RCMR requires) was run on a 4-processor implementation, and the added computational burden of RCMR was about 1%. Similar comments can be made in comparing RCMR to data assimilation codes based on adjoint methods [30]; in fact, RCMR does not require an adjoint model, and none exists for GITM.

Beyond state estimation, data assimilation techniques can be used for model refinement in the case of parameter estimation. The classical approach is to use the extended Kalman filter [31]. Along the same lines, particle filter techniques, ensemble methods, sigma point filters, and Fokker-Planck solvers [32, 33, 34, 35, 36, 37] can be used to estimate constant and time-varying parameters modeled as fictitious states. These techniques can also be used to compensate for (but not correct) model deficiencies due to numerical discretization, parameter errors, and uncertain physics [38]. All of these techniques generate statistical measures of the accuracy of the parameter estimates and thus rely on prior statistical information and require an ensemble of models. Consequently, these techniques tend to be computationally expensive. In addition, RCMR treats the parameter estimation problem as an inherently linear problem, which makes RCMR suitable for estimating large numbers of uncertain parameters. Finally, RCAC has the ability to update high-order dynamic models.

7. Retrospective Cost Adaptive Input Estimation

State estimation techniques, such as the Kalman filter and its variants, use measurements to recursively refine state estimates. The input to the system is typically modeled as a combination of an unknown zero-mean stochastic signal and a known deterministic signal. The deterministic signal is injected numerically into the observer, thereby enhancing the accuracy of the estimated states. In practice, however, the deterministic input may be unknown, and treating this signal as part of the stochastic input may yield poor state estimates. Consequently, extensive research has been devoted to developing state estimators that are either insensitive to the lack of knowledge of the deterministic input or attempt to estimate this signal along with the states. These techniques are referred to as unbiased Kalman filters, unknown input observers, and state estimators with input reconstruction [39, 40, 41, 42, 43, 44, 45, 46, 47, 48]. The ability to estimate inputs is crucial to applications where the system is strongly driven and entrainment effects are the overriding phenomenon [49, 50, 51].

Retrospective cost adaptive input estimation was demonstrated in [52]. The paper demonstrates the core of the retrospective cost approach, namely, the ability to adaptively estimate the input to a system, which may be either an external or internal signal (in the case of a subsystem). This technique forms the basis for estimating the signal \hat{u} in Figure 1(b).

8. Case Study: Retrospective Cost State and Input Estimation for GITM

We now present a case study where the goal is to estimate the unknown input to a system. This objective supports the goals of DDDAS by enhancing prediction accuracy. In particular, state and input estimation are considered in [22] based on the 3D GITM model with both synthetic and real measurements. Here we consider the case of real measurements from the CHAMP satellite.

This study is motivated by the fact that radio propagation and satellite drag are affected by the Sun's influence on the ionosphere and thermosphere. In particular, extreme ultraviolet (EUV) and X-ray radiation produce photoionization, which, in turn, through chemistry and heating, drives the formation of the ionosphere and shapes the thermosphere. In addition, the effect of the EUV and X-ray radiation is sufficient to render the ionosphere-thermosphere a strongly driven system [49, 50, 51].

Since a significant portion of EUV and X-ray radiation is absorbed by the atmosphere, it is not possible to measure these quantities from the ground. Instead, a proxy is used. The most common proxy for EUV and X-ray radiation is the flux solar irradiance at a wavelength of 10.7 nm ($F_{10.7}$), which is measured (in units of 10^{-22} W Hz⁻¹ m⁻² = 1 solar flux unit (SFU)) by the Dominion radio observatory in Penticton, Canada [53]. A shortcoming of this technique is that $F_{10.7}$ does not have a one-to-one correlation with each of the wavelengths in the EUV and X-ray bands, and thus the measured $F_{10.7}$ is often a misrepresentation of the true solar spectrum.

Although our ultimate goal is to estimate the true flux in multiple EUV and X-ray wavelength bins, a more attainable intermediate goal is to estimate the value of $F_{10.7}$ that best characterizes the ionosphere and thermosphere. The ability to estimate $F_{10.7}$ from alternative measurements can provide a cross check on the available measurements, while also providing an illustrative proof-of-concept demonstration of RCASE as a first step toward estimating X-ray and EUV in multiple bands. Furthermore, current models do not fully capture the dynamics of the ionosphere-thermosphere, in which case $F_{10.7}$ can be used as an input to the model in order to eliminate the errors between real measurements and synthetic (simulated) measurements. This study thus attempts to specify $F_{10.7}$ based on simulated measurements of the atmosphere as well as with real satellite data. The specified $F_{10.7}$ can then be used to obtain improved estimates of the state of the ionosphere and thermosphere globally and possibly predict its future evolution. This is a problem of state and input estimation.

To estimate $F_{10.7}$, we use the Global Ionosphere Thermosphere Model (GITM) [24]. GITM simulates the density, temperature, and winds in the thermosphere and ionosphere across the globe from 100 km to 600 km altitude, depending on the solar conditions at the time. The main inputs to GITM are the high-latitude electrodynamics (i.e., the aurora and the associated electric fields), tides from the lower atmosphere, and the brightness of the sun at various wavelengths, which can be proxied through the use of $F_{10.7}$. GITM solves for the chemistry, dynamics, and thermodynamics of the upper atmosphere self-consistently by accounting for interactions among various species of ions and neutrals.

In [22] we used the retrospective cost adaptive state estimation (RCASE) technique [28] to estimate the unknown solar driver $F_{10.7}$ using the Global Ionosphere-Thermosphere Model and satellite measurements. RCASE assumes that the input to the system is unknown, and uses retrospective optimization to construct an input to the adaptive estimator that minimizes the retrospective cost function. The retrospectively optimized input is then used to asymptotically drive the error between the measured output and the estimator output to zero. In this way, RCASE asymptotically estimates the unknown input to the system and the unknown states of the system. A useful feature of RCASE is that an explicit nonlinear or linearized model is not required. In addition, unlike ensemble-based data-assimilation algorithms [32, 33, 34], RCASE uses only one copy of the system model and thus is ensemble-free.

For the case of real satellite data case, the neutral mass density data measured by CHAMP (the “truth data”) is labeled $y(k)$, while the neutral mass density data measured by GRACE is labeled $y_G(k)$. First, we run GITM with the measured $\bar{F}_{10.7}(k)$ and record the neutral mass density at CHAMP locations and GRACE locations, which are labeled $\hat{y}_m(k)$ and $\hat{y}_{G,m}(k)$, respectively. Next, we combine RCASE and GITM, and use $y(k)$ to estimate $\bar{F}_{10.7}(k)$ and states. The neutral mass density output from GITM with RCASE at CHAMP and GRACE locations are labeled $\hat{y}(k)$ and $\hat{y}_G(k)$, respectively. Note that data from GRACE are used only as a metric for assessing the accuracy of state estimates, and are not used by RCASE. We further divide this setup into two cases. First, in RCASE, we use GITM with photoelectron heating. When photoelectron heating is used in GITM, then the neutral density output from GITM at CHAMP locations using measured $\bar{F}_{10.7}(k)$ closely matches CHAMP neutral density measurements. However, it should be noted that the photoelectron heating efficiency coefficient that yields low error between GITM and CHAMP is obtained by trial and error, and cannot be calculated or measured. In the second case, in RCASE, we use GITM without photoelectron heating. In this case, GITM with measured $\bar{F}_{10.7}(k)$ yields a large error between the outputs from GITM at CHAMP locations and CHAMP measurements. In this case, RCASE will use $\hat{\bar{F}}_{10.7}(k)$ as an input to GITM in order to correct the errors between CHAMP measurements and the output from GITM at CHAMP locations, and thus account for the inaccuracies incurred by removing photoelectron heating from GITM.

Let $p(k) \in \mathbb{R}$ be an arbitrary signal, and let T be a positive integer. Then, for all $k \geq T$, define the windowed average of the signal $p(k)$ as

$$\mu_{T,p}(k) \triangleq \frac{1}{T} \sum_{i=k-T+1}^k p(i),$$

where T is the interval over which the signal is averaged. Similarly, for all $k \geq T$, define the windowed standard deviation of the signal $p(k)$ as

$$\sigma_{T,p}(k) \triangleq \sqrt{\frac{1}{T} \sum_{i=k-T+1}^k (p(i) - \mu_{T,p}(i))^2}.$$

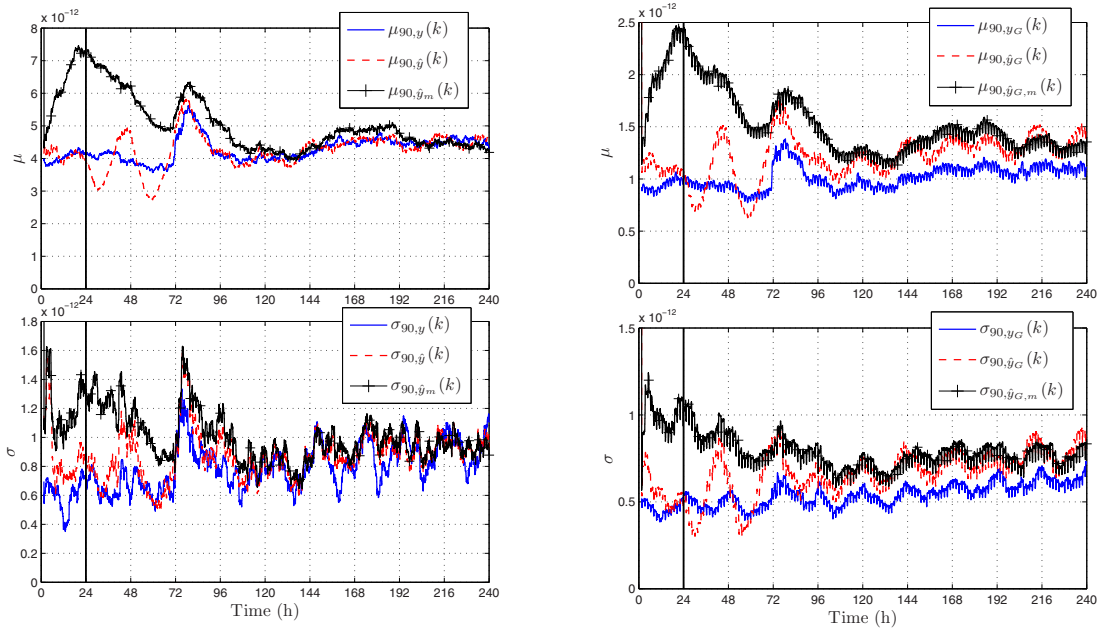
The root mean square value of $p(k)$ is denoted by $\text{RMS}(p)$.

When GITM is used with RCASE, we keep $\hat{\bar{F}}_{10.7}(k)$ at a constant value of 100 SFU for the first 24 h, after which RCASE is turned on. This allows the response due to initial conditions to decay significantly. We implement GITM on four processors with a resolution of 5° latitude by 5° longitude. The time step for GITM is set at 2 sec, and RCASE is used to update $\hat{\bar{F}}_{10.7}(k)$ every 60 sec. In all figures in this section, the vertical black line indicates when RCASE is switched on. Finally, the numerical experiments consider the period from 2002-11-24 to 2002-12-06.

We consider the case where the truth data are recorded by CHAMP from 2002-11-24 to 2002-12-06 and we use GITM with photoelectron heating. We calculate the RMS of $z(k)$ after 144 h in order to minimize the effect of transients in $\hat{y}(k)$ generated during the convergence of the adaptive subsystem. First, we consider the measurements from CHAMP. Figure 4(a) shows the windowed mean and variance of $y(k)$, $\hat{y}(k)$, and $\hat{y}_m(k)$. For this example, GITM with measured $\bar{F}_{10.7}(k)$ yields $\text{RMS}(z) = 6.5 \times 10^{-13}$, and GITM with RCASE yields $\text{RMS}(z) = 6.1 \times 10^{-13}$. In other words, GITM with RCASE yields 6% reduction in $\text{RMS}(z)$ compared to GITM with measured $\bar{F}_{10.7}(k)$.

Figure 5 shows the measured and estimated $\bar{F}_{10.7}(k)$. This plot shows that $\mu_{1440, \hat{\bar{F}}_{10.7}}(k)$ (the average of $\hat{\bar{F}}_{10.7}(k)$ over 1 day) converges to within 6 SFU of the measured values of $\bar{F}_{10.7}(k)$ in 72 h.

Finally, we consider data from GRACE to assess the quality of the state estimates. Define $z_G(k) \triangleq y_G(k) - \hat{y}_G(k)$. Figure 4(b) shows the windowed mean and variance of $y_G(k)$, $\hat{y}_G(k)$, and $\hat{y}_{G,m}(k)$. For this example, GITM with measured $\bar{F}_{10.7}(k)$ yields $\text{RMS}(z_G) = 4 \times 10^{-13}$, whereas GITM with RCASE yields $\text{RMS}(z_G) = 3.6 \times 10^{-13}$. Therefore, GITM with RCASE yields 11% reduction in $\text{RMS}(z_G)$ compared to GITM with measured $\bar{F}_{10.7}(k)$.



(a) Output-matching performance of RCASE for GITM using driver estimates.

(b) State-estimation performance of RCASE for GITM.

Fig. 4. (a) $\mu_{90,y}(k)$, $\mu_{90,\hat{y}}(k)$, $\mu_{90,\hat{y}_m}(k)$, $\sigma_{90,y}(k)$, $\sigma_{90,\hat{y}}(k)$, and $\sigma_{90,\hat{y}_m}(k)$ for the case of real CHAMP satellite data and GITM with photoelectron heating. For this example, GITM with RCASE yields 6% lower $\text{RMS}(z)$ compared to GITM with measured $\bar{F}_{10.7}(k)$. (b) This plot shows $\mu_{90,y_G}(k)$, $\mu_{90,\hat{y}_G}(k)$, $\mu_{90,\hat{y}_{G,m}}(k)$, $\sigma_{90,y_G}(k)$, $\sigma_{90,\hat{y}_G}(k)$, and $\sigma_{90,\hat{y}_{G,m}}(k)$ for real GRACE satellite data and the case of real CHAMP satellite data and GITM with photoelectron heating. For this example, GITM with RCASE yields 11% reduction in $\text{RMS}(z_G)$ compared to GITM with measured $\bar{F}_{10.7}(k)$.

9. Extensions to Nonlinear Models

To ascertain subsystem model order, RCMR can be run with various model orders, and the spectral content of the error signal can be used to determine whether the dynamic order of the Unknown Subsystem Model is sufficiently high for representing the dynamics of the Unknown Physical Subsystem. This can easily be done by varying the order of the linear Unknown Subsystem Model. However, many applications require that RCMR have the ability to represent a large class of *nonlinear* Unknown Subsystem Models. This can be done in the following way. In RCMR, the Unknown Subsystem Model has the form of an ARMAX time series model, where the next output $\hat{u}(k + 1)$ is a function of the previous outputs $\hat{u}(k - i)$ and past inputs $\hat{y}(k - j)$. RCMR uses a regression technique to update the coefficients of this model. However, this technique can be applied to *nonlinear* functions of the past outputs and inputs. The resulting nonlinear ARMAX model (called a NARMAX model) provides a rich class of model structures that can enable the search for efficient and accurate subsystem models.

NARMAX models have been used extensively for nonlinear system identification [54, 55, 56, 57, 58, 59, 60], and they can be used within RCMR to represent the Unknown Subsystem Model [61, 61]. To do this, it is necessary to examine the effectiveness of various basis functions such as radial basis functions and wavelets, which can be used by RCMR for constructing NARMAX representations of the Unknown Subsystem Model.

Acknowledgments

This research was supported in part by AFOSR DDDAS grant FA9550-12-1-0401, NSF CDI grant AGS-1027192, and NSF CPS grant CNS-1035236.

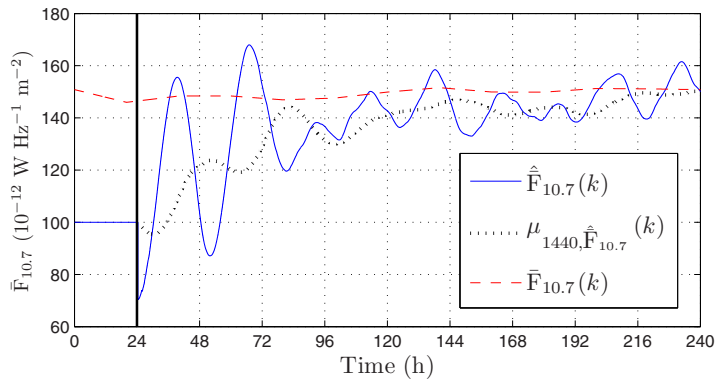


Fig. 5. Measured and estimated $\hat{F}_{10.7}(k)$ for the case of real CHAMP satellite data and GITM with photoelectron heating. This plot shows that $\mu_{1440, \hat{F}_{10.7}}(k)$ (the average of $\hat{F}_{10.7}(k)$ over 1 day) converges to within 6 SFU of the measured values of $\hat{F}_{10.7}(k)$ in 72 h.

References

- [1] G. Cruz, A. M. D'Amato, D. S. Bernstein, Retrospective cost adaptive control of spacecraft attitude, in: Proc. AIAA Guid. Nav. Contr. Conf., Minneapolis, MN, 2012, AIAA-2012-4624-236.
- [2] A. M. D'Amato, E. D. Sumer, D. S. Bernstein, Frequency-domain stability analysis of retrospective-cost adaptive control for systems with unknown nonminimum-phase zeros, in: Proc. Conf. Dec. Contr., Orlando, FL, 2011, pp. 1098–1103.
- [3] Y.-C. Cho, J. B. Hoagg, D. S. Bernstein, W. Shyy, Retrospective Cost Adaptive Flow Control of Low-Reynolds Number Aerodynamics Using a Dielectric Barrier Discharge Actuator, in: Proc. 5th AIAA Flow Contr. Conf., Chicago, IL, 2010, aIAA-2010-4841.
- [4] R. J. Fuentes, J. B. Hoagg, B. J. Anderton, A. M. D'Amato, D. S. Bernstein, Investigation of Cumulative Retrospective Cost Adaptive Control for Missile Application, in: AIAA Guid. Nav. Contr. Conf., Toronto, 2010, aIAA 2010-7577.
- [5] M. A. Santillo, D. S. Bernstein, Adaptive Control Based on Retrospective Cost Optimization, AIAA J. Guid. Contr. Dyn. 33 (2010) 289–304.
- [6] J. B. Hoagg, D. S. Bernstein, Retrospective Cost Model Reference Adaptive Control for Nonminimum-Phase Systems, AIAA J. Guid. Contr. Dyn. 35 (2012) 1767–1786.
- [7] R. Venugopal, D. S. Bernstein, Adaptive Disturbance Rejection Using ARMARKOV System Representations, IEEE Trans. Contr. Sys. Tech. 8 (2000) 257–269.
- [8] J. B. Hoagg, M. A. Santillo, D. S. Bernstein, Discrete-time Adaptive Command Following and Disturbance Rejection with Unknown Exogenous Dynamics, IEEE Trans. Autom. Contr. 53 (2008) 912–928.
- [9] H. Sane, R. Venugopal, D. S. Bernstein, Disturbance Rejection Using Self-Tuning ARMARKOV Adaptive Control with Simultaneous Identification, IEEE Trans. Contr. Sys. Tech. 19 (2001) 101–106.
- [10] O. Nelles, Nonlinear System Identification, Springer, 2001.
- [11] L. Ljung, T. Soderstrom, Theory and Practice of Recursive Identification, The MIT Press, 1983.
- [12] L. Ljung, System Identification: Theory for the User, 2nd Edition, Prentice Hall Information and System Sciences Series, Prentice Hall, 1999.
- [13] J.-N. Juang, Applied System Identification, Prentice Hall, 1993.
- [14] P. Van Overschee, B. De Moor, Subspace Identification for Linear Systems: Theory, Implementation, Applications, Kluwer, 1996.
- [15] T. Soderstrom, P. Stoica, System Identification, Prentice Hall, 1989.
- [16] R. Haber, L. Keviczky, Nonlinear System Identification—Input-Output Modeling Approach, Vol. 1: Nonlinear System Parameter Identification, Kluwer Academic Publishers, 1999.
- [17] A. M. D'Amato, A. J. Ridley, D. S. Bernstein, Retrospective-cost-based adaptive model refinement for the ionosphere and thermosphere, Statistical Analysis and Data Mining 4 (2011) 446–458.
- [18] A. M. D'Amato, B. J. Arritt, J. A. Banik, E. V. Ardelean, D. S. Bernstein, Structural health determination and model refinement for a deployable composite boom, in: Proc. AIAA SDM Conf., Palm Springs, CA, 2009, AIAA-2009-2373.
- [19] J. Yan, A. M. D'Amato, D. Sumer, J. B. Hoagg, D. S. Bernstein, Adaptive control of uncertain hammerstein systems with monotonic input nonlinearities using auxiliary nonlinearities, in: Proc. Conf. Dec. Contr., Maui, HI, 2012, pp. 4811–4816.
- [20] G. Cruz, A. M. D'Amato, D. S. Bernstein, Retrospective cost adaptive control of spacecraft attitude, in: Proc. AIAA Guid. Nav. Contr. Conf., Minneapolis, MN, 2012, aIAA-2012-4624-236.
- [21] J. Yan, A. M. D'Amato, K. Butts, I. Kolmanovsky, D. S. Bernstein, Adaptive control of the air flow system in a diesel engine, in: Proc. DSCC, Fort Lauderdale, FL, 2012, DSCC2012-MOVIC2012-8597.
- [22] A. A. Ali, K. Agarwal, A. J. Ridley, D. S. Bernstein, Ensemble-Free State and Driver Estimation in the Ionosphere-Thermosphere Using Retrospective-Cost-Based Adaptive Estimation(submitted).
- [23] A. M. D'Amato, J. Forman, T. Ersal, A. A. Ali, J. Stein, H. Peng, D. S. Bernstein, Noninvasive battery-health diagnostics using retrospective-cost identification of inaccessible subsystems, in: Proc. DSCC, Fort Lauderdale, FL, 2012, dSCC2012-MOVIC2012-8649.
- [24] A. J. Ridley, Y. Deng, G. Töth, The global ionosphere-thermosphere model, J. Atmos. Sol-Terr. Phys. 68 (2006) 839–864.
- [25] R. G. Roble, E. C. Ridley, A. D. Richmond, R. E. Dickinson, A coupled thermosphere/ionosphere general circulation model, Geophys. Res. Lett. 15 (12) (1988) 1325–1328.

- [26] C. A. Barth, K. D. Mankoff, S. M. Bailey, S. C. Solomon, Global observations of nitric oxide in the thermosphere, *J. Geophys. Res.* 108(A1) (2003) 1027.
- [27] D. R. Marsh, S. C. Solomon, A. E. Reynolds, Empirical model of nitric oxide in the lower thermosphere, *J. Geophys. Res.* 109 (2004) A07301.
- [28] A. M. D'Amato, J. Springmann, A. A. Ali, J. W. Cutler, A. J. Ridley, D. S. Bernstein, Adaptive state estimation for nonminimum-phase systems with uncertain harmonic inputs, in: *Proc. AIAA Guid. Nav. Contr. Conf.*, Portland, OR, 2011, aIAA-2011-6315.
- [29] G. Evensen, The ensemble kalman filter: theoretical formulation and practical implementation, *Ocean Dynamics* 53 (2003) 343–367.
- [30] A. Caya, J. Sun, C. Snyder, A Comparison between the 4DVAR and the Ensemble Kalman Filter Techniques for Radar Data Assimilation, *Monthly Weather Rev.* 133 (2005) 3081–3094.
- [31] L. Ljung, Asymptotic behavior of the extended kalman filter as a parameter estimator for linear systems, *IEEE Trans. Autom. Control* 24 (1979) 36–50.
- [32] P. L. Houtekamer, H. L. Mitchell, Data assimilation using an ensemble Kalman filter technique, *Monthly Weather Review* 126 (1998) 796–811.
- [33] G. Evensen, Sequential data assimilation with a nonlinear quasi-geostrophic model using monte carlo methods to forecast error statistics, *J. Geophys. Res.* 99 (1994) 10,143–10,162.
- [34] J. L. Anderson, An ensemble adjustment Kalman filter for data assimilation, *Monthly Weather Review* 129 (2001) 2884–2903.
- [35] G. Terejanu, P. Singla, T. Singh, P. Scott, Adaptive Gaussian Sum Filter for Nonlinear Bayesian Estimation, *IEEE Transactions on Automatic Control* 56 (2011) 2151–2156.
- [36] M. Kumar, S. Chakravorty, P. Singla, J. L. Junkins, The Partition of Unity Finite Element Approach with hp-refinement to the Stationary Fokker-Planck Equation, *Journal of Sound and Vibration* 327 (2009) 144–162.
- [37] S. Julier, J. Uhlmann, H. Durrant-Whyte, A new method for the nonlinear transformation of means and covariances in filters and estimators, *IEEE Trans. Autom. Control* 45 (2000) 477–482.
- [38] H. C. Godinez, J. Koller, Localized adaptive inflation in ensemble data assimilation for a radiation belt model, *Space Weather* 10 (2012) 1–11, doi:10.1029/2012SW000767.
- [39] S. Bhattacharyya, Observer design for linear systems with unknown inputs, *IEEE Trans. Autom. Control* 23 (1978) 483–484.
- [40] P. K. Kitaniadis, Unbiased minimum-variance linear state estimation, *Automatica* 23 (1987) 775–778.
- [41] S. Gillijns, B. De Moor, Unbiased minimum-variance input and state estimation for linear discrete-time systems, *Automatica* 43 (1) (2007) 111–116.
- [42] M. Hou, P. Muller, Design of observers for linear systems with unknown inputs, *IEEE Trans. Autom. Control* 37 (1992) 871–875.
- [43] M. E. Valcher, State observers for discrete-time linear systems with unknown inputs, *IEEE Trans. Autom. Control* 44 (1999) 397–401.
- [44] Y. Xiong, M. Saif, Unknown disturbance inputs estimation based on a state functional observer design, *Automatica* 39 (2003) 1389–1398.
- [45] T. Floquet, J. P. Barbot, State and unknown input estimation for linear discrete-time systems, *Automatica* 44 (2006) 1883–1889.
- [46] S. Sundaram, C. N. Hadjicostis, Delayed observers for linear systems with unknown inputs, *IEEE Trans. Autom. Control* 52 (2007) 334–339.
- [47] H. J. Palanhandalam-Madapusi, D. S. Bernstein, Unbiased minimum-variance filtering for input reconstruction, in: *Proc. Amer. Contr. Conf.*, New York City, NY, 2007, pp. 5712–5717.
- [48] S. Kirtikar, H. Palanhandalam-Madapusi, E. Zattoni, D. S. Bernstein, l -delay input and initial-state reconstruction for discrete-time linear systems, *Circ. Sys. Sig. Processing* 30 (2011) 233–262.
- [49] D. Angeli, A Lyapunov approach to incremental stability properties, *IEEE Trans. Autom. Control* 47 (2002) 410–421.
- [50] G. Russo, M. di Bernardo, E. D. Sontag, Global entrainment of transcriptional systems to periodic inputs, *PLOS Computational Biology* 6 (2010) 1–26.
- [51] E. Sontag, Contractive systems with inputs, in: J. C. Willems, S. Hara, Y. Ohta, H. Fujioka (Eds.), *Perspectives in Mathematical System Theory, Control, and Signal Processing*, Vol. 398, Springer, 2010, pp. 217–228.
- [52] A. M. D'Amato, D. S. Bernstein, Adaptive forward-propagation input reconstruction for nonminimum-phase systems, in: *Proc. Amer. Contr. Conf.*, Montreal, 2012, pp. 598–603.
- [53] National Research Council Canada, Dominion radio astrophysical observatory, [accessed 6-February-2013] (2012). URL <https://www.astrosci.ca/DA0/>
- [54] S. A. Billings, Identification of nonlinear systems—a survey, *IEE Proc.* 127 (6) (1980) 272–285.
- [55] S. Chen, S. A. Billings, Representation of nonlinear systems: The narmax model, *Int. J. Contr.* 49 (1989) 1013–1032.
- [56] S. Chen, S. A. Billings, C. F. N. Cowan, P. M. Grant, Practical identification of narmax models using radial basis function, *Int. J. Contr.* 52 (1990) 1327–1350.
- [57] H. L. Wei, S. A. Billings, M. A. Balikhin, Wavelet based non-parametric narx models for nonlinear inputoutput system identification, *International Journal of Systems Science* 37 (2006) 1089–1096.
- [58] M. A. Balikhin, R. J. Boynton, S. A. Billings, M. Gedalin, N. Ganushkina, D. Coca, H. Wei, Data based quest for solar wind—magnetosphere coupling function, *J. Geophysical Res.* 37, doi:10.1029/2010GL045733.
- [59] R. J. Boynton, M. A. Balikhin, S. A. Billings, H. L. Wei, N. Ganushkina, Using the NARMAX OLS-ERR algorithm to obtain the most influential coupling functions that affect the evolution of the magnetosphere, *J. Geophysical Res.* 116, doi:10.1029/2010JA015505.
- [60] M. A. Balikhin, R. J. Boynton, S. N. Walker, J. E. Borovsky, S. A. Billings, H. L. Wei, Using the NARMAX approach to model the evolution of energetic electrons fluxes at geostationary orbit, *J. Geophysical Res.* 38, doi:10.1029/2011GL048980.
- [61] J. Yan, A. M. D'Amato, D. S. Bernstein, Retrospective-cost adaptive control of uncertain hammerstein systems using a narmax controller structure, in: *Proc. AIAA Guid. Nav. Contr. Conf.*, Minneapolis, MN, 2012, AIAA-2012-4448-132.